$g-2$ of charged leptons, $\alpha(M_Z^2)$, and the hyperfine splitting of muonium

Alexander Keshavarzi [1,2,*] Daisuke Nomura,[3,†] and Thomas Teubner [4,‡]

[1]*Department of Physics and Astronomy, The University of Manchester,*
Manchester M13 9PL, United Kingdom
[2]*Department of Physics and Astronomy, The University of Mississippi, Mississippi 38677, USA*
[3]*KEK Theory Center, Tsukuba, Ibaraki 305-0801, Japan*
[4]*Department of Mathematical Sciences, University of Liverpool,*
Liverpool L69 3BX, United Kingdom

Following updates in the compilation of $e^+e^- \to$ hadrons data, this work presents reevaluations of the hadronic vacuum polarization contributions to the anomalous magnetic moments of the electron (a_e), muon (a_μ) and tau lepton (a_τ), to the ground-state hyperfine splitting of muonium and also updates the hadronic contributions to the running of the QED coupling at the mass scale of the Z boson, $\alpha(M_Z^2)$. Combining the results for the hadronic vacuum polarization contributions with recent updates for the hadronic light-by-light corrections, the electromagnetic and the weak contributions, the deviation between the measured value of a_μ and its Standard Model prediction amounts to $\Delta a_\mu = (28.02 \pm 7.37) \times 10^{-10}$, corresponding to a muon $g-2$ discrepancy of 3.8σ.

I. INTRODUCTION

For the charged leptons ($l = e, \mu, \tau$), the study of their anomalous magnetic moment, $a_l = (g-2)_l/2$, continues to serve as a long-standing test of the Standard Model (SM) and as a powerful indirect search for new physics. In each case, the SM prediction of the anomalous magnetic moment is determined by summing the contributions from all sectors of the SM, such that

$$a_l^{SM} = a_l^{QED} + a_l^{EW} + a_l^{had,VP} + a_l^{had,LbL}, \quad (1.1)$$

where a_l^{QED} are the QED contributions, a_l^{EW} are the (electro) weak (EW) contributions, $a_l^{had,VP}$ are the hadronic (had) vacuum polarization (VP) contributions and $a_l^{had,LbL}$ are those contributions due to hadronic light-by-light (LbL) scattering.

The recent complete reevaluation of the hadronic VP contributions to a_μ preceding this work (denoted as KNT18) found the SM prediction to be $a_\mu^{SM}(\text{KNT18}) =$

$(11\,659\,182.04 \pm 3.56) \times 10^{-10}$ [1], with the uncertainty still entirely dominated by the nonperturbative, hadronic sector. Compared with the current experimental world average of $a_\mu^{exp} = (11\,659\,209.1 \pm 6.3) \times 10^{-10}$ [2–5], a discrepancy of $\Delta a_\mu = a_\mu^{exp} - a_\mu^{SM} = (27.06 \pm 7.26) \times 10^{-10}$ was found, with the SM prediction being 3.7σ below the experimental measurement. With new efforts at Fermilab (FNAL) [6,7] (and later at J-PARC [8]) aiming to reduce the experimental uncertainty by a factor of 4, coupled with the ongoing efforts of the Muon $g-2$ Theory Initiative [9] to improve the determination of the various SM contributions in conjunction with these new measurements, it is imperative that the determination in Ref. [1] be continuously updated and improved.

A relatively new and interesting deviation has now also arisen in the study of the electron $g-2$. Until recently, the comparison of the exceptionally precise measurement of $a_e^{exp} = (1\,159\,652\,180.73 \pm 0.28) \times 10^{-12}$ [10] with the SM prediction $a_e^{SM}(\alpha_{Rb}) = (1\,159\,652\,182.032 \pm 0.720) \times 10^{-12}$ [11] (which updated Ref. [12]) deviated only at the level of 1.7σ. Here, α_{Rb} denotes that the SM prediction has been determined using the measurement of the fine-structure constant via rubidium (Rb) atomic interferometry [13], which contributes the dominant uncertainty to this prediction of a_e^{SM}. However, the use of a new, more precise measurement of α using cesium (Cs) atomic interferometry [14] results in an estimate of $a_e^{SM}(\alpha_{Cs}) = (1159652181.61 \pm 0.23) \times 10^{-12}$. This implies a deviation of $\Delta a_e = a_e^{exp} - a_e^{SM}(\alpha_{Cs}) = (-0.88 \pm 0.36) \times 10^{-12}$, corresponding to a

*alexander.keshavarzi@manchester.ac.uk
†dnomura@post.kek.jp
‡thomas.teubner@liverpool.ac.uk

2.5σ difference.[1] This result has invoked much theoretical work into the possibility of simultaneously explaining the differences in both the electron and muon sector, which must also explain the current sign difference seen between Δa_e and Δa_μ (see e.g., Ref. [16]). Although, due to the small mass of the electron, a_e^{SM} is less sensitive to strong effects than a_μ^{SM}, the recently observed changes in the electron sector make it important that the hadronic contributions to the electron $g-2$ are also updated from the previous determination in Ref. [17] (denoted here as NT12).

Measurements of the anomalous magnetic moment of the tau lepton, a_τ^{exp}, are notoriously difficult due to the short lifetime of the τ and, as such, no direct measurement of a_τ has yet been achieved. Limits on a_τ^{exp} were set by the DELPHI Collaboration to be $-0.052 < a_\tau^{exp} < 0.013$ at the 95% confidence level [2,18], which is quoted in the form $a_\tau^{exp} = -0.018(17)$ in Ref. [18]. By standard lepton mass-scaling arguments, a_τ is more sensitive to heavy new physics than a_μ by a factor of $m_\tau^2/m_\mu^2 \sim 280$. However, the relative contributions of strong effects compared to both the electron and the muon make a_τ more sensitive to hadronic contributions by the same argument. The hadronic VP contributions were determined in Ref. [19] to be $a_\tau^{had,VP} = (345.1 \pm 3.9) \times 10^{-8}$, resulting (along with calculations of the various other SM contributions) in $a_\tau^{SM} = (117721 \pm 5) \times 10^{-8}$. Although it is clear that the comparison of $\Delta a_\tau = a_\tau^{exp} - a_\tau^{SM}$ is insignificant due to the current insufficient accuracy of a_τ^{exp}, the determination of a_τ^{SM} is an interesting undertaking and may prove useful, should experimental techniques improve to be able to better probe the anomaly of the τ lepton.

It follows that this work, denoted KNT19, will update the hadronic vacuum polarization contributions to $a_l = (g-2)_l/2$ for all $l = e, \mu, \tau$. These are calculated utilizing dispersion integrals and the experimentally measured cross section,

$$\sigma_{had,\gamma}^0(s) \equiv \sigma^0(e^+e^- \to \gamma^* \to hadrons + \gamma), \quad (1.2)$$

where the superscript 0 denotes the bare cross section (undressed of all vacuum polarization effects) and the subscript γ indicates the inclusion of effects from final-state radiation of (one or more) photons (see Ref. [1] for details). The determination of the hadronic R-ratio, defined as

$$R(s) = \frac{\sigma_{had,\gamma}^0(s)}{\sigma_{pt}(s)} \equiv \frac{\sigma_{had,\gamma}^0(s)}{4\pi\alpha^2/(3s)} \quad (1.3)$$

and obtained from the updated compilation of all available $e^+e^- \to hadrons$ data, is the foundation of this endeavor. Here, $\alpha = \alpha(0)$ is the fine-structure constant. From this, the leading-order (LO) hadronic VP contributions to a_l can be determined via the dispersion relation

$$a_l^{had,LO\,VP} = \frac{\alpha^2}{3\pi^2} \int_{s_{th}}^\infty \frac{ds}{s} R(s) K_l(s), \quad (1.4)$$

where $s_{th} = m_\pi^2$ and $K_l(s)$ is a well-known kernel function [20,21]. Expressed in the form $\hat{K}_l(s) \equiv 3s/m_l^2 K(s)$, $\hat{K}_l(s)$ is a monotonically increasing function that behaves as $\hat{K}_l(s) \to 1$ as $s \to \infty$. This behavior differs slightly for each lepton. In the case of the electron, the deviation of $\hat{K}_e(s)$ from 1 is almost negligible for all s and causes $a_e^{had,LO\,VP}$ to be heavily dominated by the contributions from the lowest energies [17]. For the muon, $K_\mu(s)$ behaves as $K_\mu(s) \sim m_\mu^2/(3s)$ at low energies and also accentuates the low-energy domain [1,22], although not as heavily as for the electron. For $\hat{K}_\tau(s)$, the larger τ mass results in a functional structure that further increases the role of contributions from higher energies relative to $\hat{K}_\mu(s)$, although the role of lower energies is still prominent [19]. At next-to-leading order (NLO), similar dispersion integrals and kernel functions exist [22,23], allowing for $a_l^{had,NLO\,VP}$ to be determined in conjunction with the LO contributions. At next-to-NLO (NNLO), $a_l^{had,NNLO\,VP}$ has been determined for $l = e, \mu$ [24].

In addition, the evaluation of the hadronic R-ratio is a crucial input for two other precision observables which test the SM. First, the hadronic contributions to the effective QED coupling $\Delta\alpha_{had}^{(5)}(q^2)$ allow for an update of this quantity at the scale of the Z boson mass, $\alpha(M_Z^2)$, which hinders the accuracy of EW precision fits. Second, the hadronic VP corrections are a non-negligible part of the ground-state hyperfine splitting (HFS) of muonium, $\Delta\nu_{Mu}$, which can be used to determine the electron-to-muon mass ratio and, hence, the muon mass.

This paper continues, in Sec. II, with a description of the updates in the compilation of hadronic cross data since [1]. Section III details the new results for the contributions to $a_l^{had,LO\,VP}$ for each $l = e, \mu, \tau$ (with corresponding new estimates for a_l^{SM}), followed by updated predictions for $\alpha(M_Z^2)$ and $\Delta\nu_{Mu}^{had,VP}$. Conclusions and discussions of future prospects are given in Sec. IV.

II. UPDATES SINCE THE LAST ANALYSIS (KNT18)

The data combination methodology in this work is unchanged from Ref. [1] and, unless differences are explicitly stated, the cross section determination for each hadronic channel is unaltered. However, various updates with respect

---

[1]Note that very recently an independent calculation of the purely photonic five-loop contributions to a_e was performed [15], which gives a different value compared to the one in Ref. [11] and which, if adopted, would slightly change the predictions for a_e^{SM} and Δa_e.
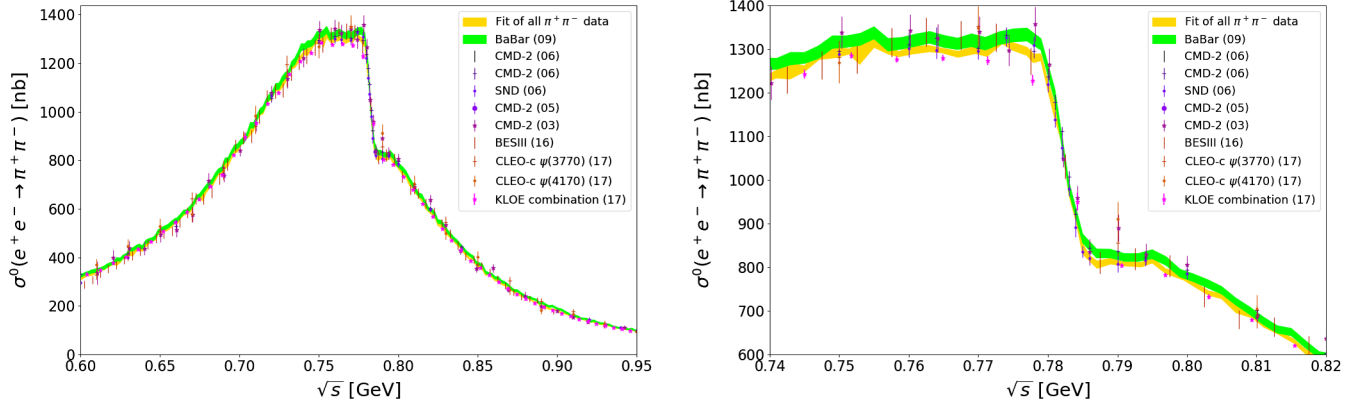
FIG. 1.   Contributing data in the ρ resonance region of the $\pi^+\pi^-$ channel plotted against the new fit of all data (left panel), with an enlargement of the ρ-ω interference region (right panel).

to the available data have been accounted for and are described in the following. As before, results for $a_\mu^{\text{had,LO VP}}$ are quoted with their respective statistical (stat) uncertainty, systematic (sys) uncertainty, vacuum polarization (vp) correction uncertainty and final-state radiation (fsr) correction uncertainty. The total (tot) uncertainty is determined from the individual sources added in quadrature.

A. $\pi^+\pi^-$ channel

The all-important $\pi^+\pi^-$ channel is modified only by the introduction of a new radiative return measurement based on data taken at the CLEO-c experiment between $0.3 \leq \sqrt{s} \leq 1.0$ GeV, covering the dominant ρ resonance region [25]. The measurement consists of two data sets: the first is taken at e^+e^- energies at the center of mass of the $\psi(3770)$ resonance and the second is at the $\psi(4170)$ resonance. Although these measurements come already undressed of VP effects as required by Eq. (1.2), the undressing procedure applied in Ref. [25] used an outdated routine [26]. Therefore, in this work, the published cross section values are redressed utilizing the routine provided in Ref. [26] and then undressed via the KNT18 vacuum polarization routine, `vp_knt_v3_0` [1,27].[2] Notably, the statistical and systematic uncertainties of the CLEO-c data are large compared to the KLOE [28–31] and BABAR [32] measurements and, therefore, cannot resolve the tension between the KLOE and BABAR data. In addition, in the KNT19 data combination, the systematic uncertainties of the two CLEO-c data sets are taken to be 100% correlated, which further limits their influence.

The combined cross section and the dominant contributing measurements are displayed in the ρ region and magnified in the ρ-ω interference region in Fig. 1. Figure 2 shows the updated comparison of the evaluations of $a_\mu^{\pi^+\pi^-}$ from the radiative return measurements and the

combination of remaining direct scan data in the vicinity of the ρ resonance. Although the new CLEO-c data are compatible with both the KLOE and BABAR measurements, resulting in a marginal improvement in the quality of the overall fit, as expected the combination is largely unchanged due to the large uncertainties of the CLEO-c data. The tension between BABAR and KLOE persists, emanated in the KNT19 combination of all $\pi^+\pi^-$ data, which is still dominated by the three KLOE cross section measurements and their precise, highly correlated uncertainties. This is further exemplified by Fig. 3, which clearly indicates the tension between KLOE and BABAR, and between the fit of all $\pi^+\pi^-$ data and BABAR, especially in the high-energy tail of the ρ resonance.

For the muon $g − 2$, the full combination of all $\pi^+\pi^-$ data gives

$$a_\mu^{\pi^+\pi^-}[0.305 \leq \sqrt{s} \leq 1.937 \text{ GeV}]$$
$$= (503.46 \pm 1.14_{\text{stat}} \pm 1.52_{\text{sys}} \pm 0.06_{\text{vp}} \pm 0.14_{\text{fsr}}) \times 10^{-10}$$
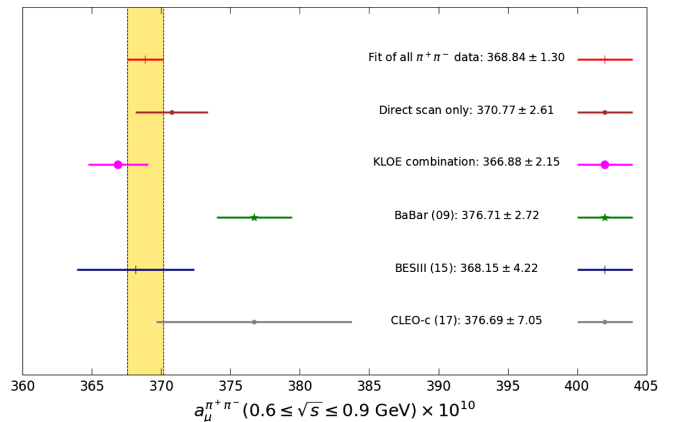$$= (503.46 \pm 1.91_{\text{tot}}) \times 10^{-10}. \tag{2.1}$$

FIG. 2.   Comparison of the evaluations of $a_\mu^{\pi^+\pi^-}$ from the individual radiative return measurements and the combination of direct scan $\pi^+\pi^-$ measurements between $0.6 \leq \sqrt{s} \leq 0.9$ GeV.

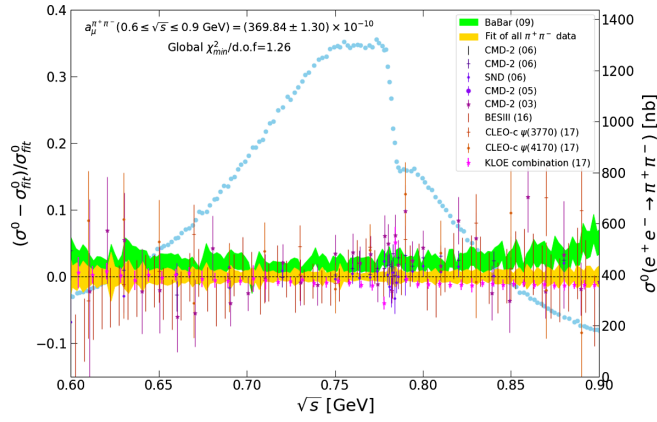[2]This routine is available for use by contacting the authors directly.

FIG. 3. The relative difference of the radiative return and the most relevant of the direct scan data sets contributing to $a_\mu^{\pi^+\pi^-}$, and the fit of all data. For comparison, the individual sets have been normalized against the fit and have been plotted in the ρ region. The green band represents the *BABAR* data and their errors (statistical and systematic, added in quadrature). The yellow band represents the full data combination which incorporates all correlated statistical and systematic uncertainties. However, the width of the yellow band simply displays the square root of the diagonal elements of the total output covariance matrix of the fit.

This value is entirely consistent with Ref. [1]. The mean value has increased by ~25% of the previous error, which itself has decreased by only ~3%. As before, tensions in the data are accounted for in the local χ^2 error inflation, increasing the uncertainty of $a_\mu^{\pi^+\pi^-}$ by ~14%. This has decreased from ~15% in Ref. [1], also reflected in the slight decrease in the global $\chi^2_{\min}/\text{d.o.f.}(\text{KNT18}) = 1.30$ to $\chi^2_{\min}/\text{d.o.f.}(\text{KNT19}) = 1.26$ (with 625 d.o.f.).

Although the results of this work are obtained from directly integrating the combined data, detailed analyses employing constraints based on analyticity and unitarity have been performed in Refs. [33–37]. These additional constraints have the potential to improve the determination of the two-pion cross section and to possibly reduce the error, especially at low energies where limited data are available. The results obtained in these works are, overall, largely compatible with the determination of this analysis, but lead to slightly larger results for $a_\mu^{\text{had,LO VP}}$ in the energy range $\sqrt{s} < 0.6$ GeV. A detailed comparison with these values is beyond the scope of this work, but will be presented as part of the studies of the Muon $g-2$ Theory Initiative [9].

B. $\pi^+\pi^-\pi^0$ channel

A recent study of the three-pion contribution to the hadronic vacuum polarization based on a global fit function using analyticity and unitarity constraints [38] highlighted major differences arising in various determinations of $a_\mu^{\pi^+\pi^-\pi^0}$. These were attributed to the choice of cross section

interpolation used in the prominent ω resonance region when integrating the data. Due to a lack of data and a (relatively) wide binning in the narrow ω resonance itself, the trapezoidal rule integration used in Refs. [1,22,39,40], while consistent with the direct data integration procedure utilized in those works, led to a value of $a_\mu^{\pi^+\pi^-\pi^0}$ in Ref. [1] larger than that found in Refs. [37,38]. In order to address this issue in this work, the clusters and covariance matrix elements corresponding to the fitted ω resonance alone have been interpolated to a 0.2 MeV binning using a quintic polynomial. The newly finer-binned resonance, along with the entire $\pi^+\pi^-\pi^0$ cross section, are then integrated using the trapezoidal rule integral to ensure consistency with the general KNT data combination procedure applied to all other channels. This results in an improved estimate of

$$a_\mu^{\pi^+\pi^-\pi^0}[0.66 \leq \sqrt{s} \leq 1.937 \text{ GeV}]$$
$$= (46.73 \pm 0.32_{\text{stat}} \pm 0.74_{\text{sys}} \pm 0.12_{\text{vp}} \pm 0.47_{\text{fsr}}) \times 10^{-10}$$
$$= (46.73 \pm 0.94_{\text{tot}}) \times 10^{-10}, \quad (2.2)$$

compared to $a_\mu^{\pi^+\pi^-\pi^0}(\text{KNT18}) = (47.79 \pm 0.89) \times 10^{-10}$ in Ref. [1]. Figure 4(a) shows an enlargement of the ω resonance region, where the comparison between the previously used trapezoidal rule integral (black dashed line), a cubic polynomial interpolation (dash-dotted green line) and the quintic polynomial (solid pink line) interpolation are visible, highlighting the improvement that this change has made.[3] It can also be seen here that while the linear interpolation clearly overestimates the resonance in the tails, the cubic interpolation seemingly underestimates and overestimates the cross section in various places in the tail, which is why the quintic polynomial was chosen. The resulting KNT19 determination of the ω resonance in the $\pi^+\pi^-\pi^0$ channel and all contributing data are shown in Fig. 4(b).

C. Other channels

There have been a number of small data updates (see Refs. [41–46]) in other channels since Ref. [1]. The affected channels are all depicted in Fig. 5 and Fig. 6. Notably, the $\pi^0\gamma$ channel now includes a new measurement from the SND experiment [41], which greatly extends the previous upper border of the channel from 1.35 to 1.935 GeV in this work. The changes to $a_\mu^{\pi^0\gamma}$ are negligible, confirming that no higher-energy contributions were missed previously in this hadronic mode.

---

[3]Should new data be released that better describe the shape of the ω resonance in this channel, the higher population of data may render this higher-order polynomial interpolation unnecessary and the trapezoidal integral over the available data may be sufficient.
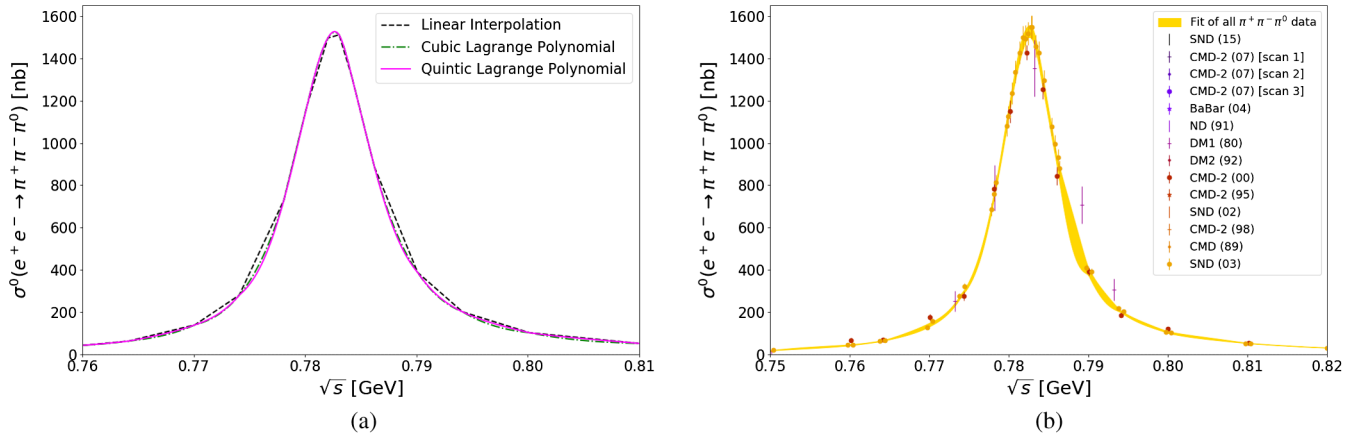
(a)

(b)

FIG. 4. The cross section $\sigma^0(e^+e^- \to \pi^+\pi^-\pi^0)$ in the region of the narrow ω resonance. In Fig. 4(a), the black dashed line, green dash-dotted line and pink solid line show the linear, cubic and quintic interpolation between clusters, respectively.

Two new channels are now included in the KNT19 data compilation. A measurement of the $2\pi^+2\pi^-\omega$ channel by CMD-3 [46] provides a negligibly small addition to $a_\mu^{\text{had,LO VP}}$. This process, together with a measurement of the

$2\pi^+2\pi^-\eta$ mode, have provided the production mechanisms to measure the seven-pion final state $3\pi^+3\pi^-\pi^0$ in the same work [46], which is the first inclusion of a final state with more than six pions. After removing the contributions from

(a) $\sigma^0(e^+e^- \to \pi\gamma)$

(b) $\sigma^0(e^+e^- \to \pi^+\pi^-\eta)$

(c) $\sigma^0\left(e^+e^- \to (\pi^+\pi^-\pi^0\eta)_{\text{no }\omega}\right)$

(d) $\sigma^0(e^+e^- \to \eta\omega)$

(e) $\sigma^0(e^+e^- \to \eta\phi)$

(f) $\sigma^0(e^+e^- \to \omega\eta\pi^0)$

(g) $\sigma^0(e^+e^- \to 2\pi^+2\pi^-\eta)$

(h) $\sigma^0(e^+e^- \to 2\pi^+2\pi^-\omega)$

(i) $\sigma^0\left(e^+e^- \to (3\pi^+3\pi^-\pi^0)_{\text{no }\eta\omega}\right)$
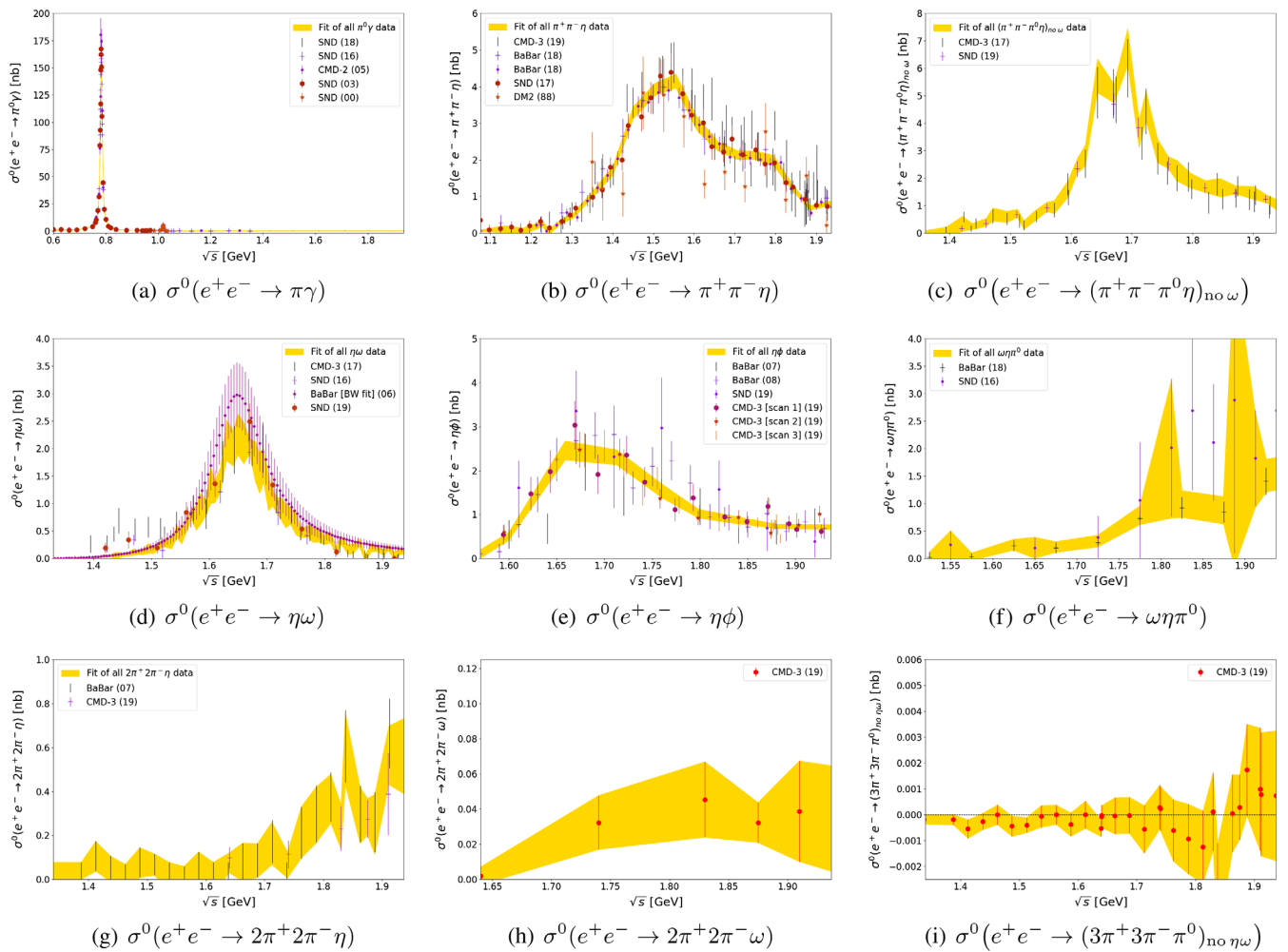
FIG. 5. The resulting cross sections of the updated, subleading hadronic channels contributing to the KNT19 data compilation.

(a) $\sigma^0\left(e^+e^- \to (\pi^+\pi^-3\pi^0)_{\mathrm{no}\,\eta}\right)$

(b) $\sigma^0(e^+e^- \to \pi^+\pi^-2\pi^0\eta)$

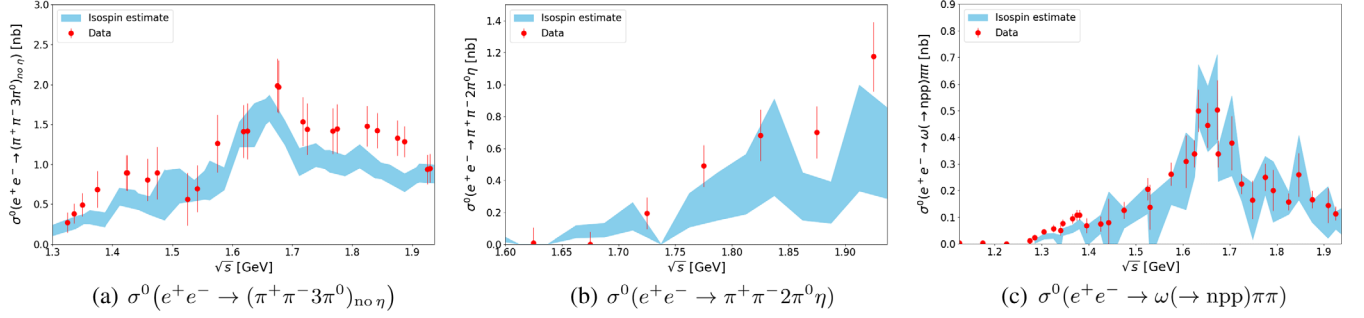(c) $\sigma^0(e^+e^- \to \omega(\to \mathrm{npp})\pi\pi)$

FIG. 6. The resulting cross sections of those hadronic channels contributing to the KNT19 data compilation that were previously estimated via isospin relations. In panel (c), the abbreviation "→ npp" represents the resonant decay to non-purely-pionic modes.

the η and ω resonances to avoid double counting, the $3\pi^+3\pi^-\pi^0$ channel is statistically consistent with zero below the upper energy boundary of the sum of exclusive states used here, i.e., 1.937 GeV. Once again, it is encouraging to verify that no large contributions were missed from these channels in the KNT18 data compilation.

Last, it is important to mention that the three modes $\pi^+\pi^-3\pi^0$, $\pi^+\pi^-2\pi^0\eta$ and $\omega\pi^0\pi^0$ that were previously unmeasured have now been measured by *BABAR* [42]. These allow, for the first time, for their corresponding hadronic contributions to be estimated using experimental data instead of previously used isospin relations. All three channels are shown in Fig. 6, where the agreement in each case between the data and the isospin prediction is good. The resulting integrated contributions to $a_\mu^{\mathrm{had,LO\,VP}}$ are all consistent with the theory estimates previously given in Ref. [1].

III. RESULTS

Table I shows the contributions of the individual hadronic channels to $a_e^{\mathrm{had,LO\,VP}}$, $a_\mu^{\mathrm{had,LO\,VP}}$, $a_\tau^{\mathrm{had,LO\,VP}}$, $\Delta\alpha_{\mathrm{had}}^{(5)}(M_Z^2)$ and $\Delta\nu_{\mathrm{Mu}}^{\mathrm{had,VP}}$ calculated in this analysis. For $a_l^{\mathrm{had,LO\,VP}}$ $(l = e, \mu, \tau)$, the combined hadronic cross section data for each channel are integrated according to Eq. (1.4). To obtain $\Delta\alpha_{\mathrm{had}}^{(5)}(M_Z^2)$, the data are integrated using Eq. (3.14) given in Sec. III D. For $\Delta\nu_{\mathrm{Mu}}^{\mathrm{had,VP}}$, Eq. (3.20) in Sec. III E is used. In the following section, the KNT19 results for a_e, a_μ, a_τ, $\alpha(M_Z^2)$ and $\Delta\nu_{\mathrm{Mu}}$ are presented separately. For each of the lepton $g-2$ results, the values for the LO and NLO hadronic VP contributions as calculated in this work are given, followed by corresponding updated estimates for the respective SM predictions and any necessary discussions.

A. The anomalous magnetic moment of the electron, a_e

Integrating the updated KNT19 determination of the hadronic R-ratio described in Sec. II according to Eq. (1.4) (with $l = e$) results in

$$a_e^{\mathrm{had,LO\,VP}} = (186.08 \pm 0.34_{\mathrm{stat}} \pm 0.53_{\mathrm{sys}}$$
$$\pm\, 0.05_{\mathrm{vp}} \pm 0.18_{\mathrm{fsr}}) \times 10^{-14}$$
$$= (186.08 \pm 0.66_{\mathrm{tot}}) \times 10^{-14}. \quad (3.1)$$

The contributions from the individual hadronic channels contributing to $a_e^{\mathrm{had,LO\,VP}}$ are listed in Table I. With the same data input, the NLO contributions to $a_e^{\mathrm{had,VP}}$ are determined here to be

$$a_e^{\mathrm{had,NLO\,VP}} = (-22.28 \pm 0.04_{\mathrm{stat}} \pm 0.06_{\mathrm{sys}} \pm 0.01_{\mathrm{vp}}$$
$$\pm\, 0.02_{\mathrm{fsr}}) \times 10^{-14}$$
$$= (-22.28 \pm 0.08_{\mathrm{tot}}) \times 10^{-14}. \quad (3.2)$$

The NT12 analysis [17] found $a_e^{\mathrm{had,LO\,VP}}(\mathrm{NT12}) = (186.6 \pm 1.1) \times 10^{-14}$ and $a_e^{\mathrm{had,NLO\,VP}}(\mathrm{NT12}) = (-22.34 \pm 0.14) \times 10^{-14}$. Comparing the results in this analysis with those from NT12, the mean values have decreased by a substantial fraction of the previously quoted uncertainties (although well within them) and the uncertainties themselves have decreased by $>40\%$. This is in line with the changes noted in the KNT18 determination of a_μ [1], which observed similar changes largely due to reductions in the mean value and uncertainty of the dominant $\pi^+\pi^-$ channel.

As the NNLO hadronic VP contributions are not calculated in this work, the result $a_e^{\mathrm{had,NNLO\,VP}} = (2.80 \pm 0.01) \times 10^{-14}$ from Ref. [24] is adopted which utilizes the HLMNT11 [40] data compilation for the hadronic R-ratio.[4] For the hadronic LbL contributions, the value $a_e^{\mathrm{had,LbL}} = (3.7 \pm 0.5) \times 10^{-14}$ from Ref. [47] is used. With these, the full hadronic contributions to the electron $g-2$ are estimated to be

$$a_e^{\mathrm{had}} = (170.30 \pm 0.77_{\mathrm{tot}}) \times 10^{-14}, \quad (3.3)$$

where, due to the complete correlations from the same input R-ratio, the errors of the hadronic VP contributions have

---

[4]During the KNT18 analysis, the authors of Ref. [24] kindly repeated their analysis with the KNT18 data compilation and found negligible changes with respect to their published result.

TABLE I. Summary of the contributions to $a_e^{\text{had,LO VP}}$, $a_\mu^{\text{had,LO VP}}$, $a_\tau^{\text{had,LO VP}}$, $\Delta\alpha_{\text{had}}^{(5)}(M_Z^2)$ and $\Delta\nu_{\text{Mu}}^{\text{had,VP}}$ calculated in this analysis. The first column indicates the channel, the second, third and fourth columns give the contributions to $a_e^{\text{had,LO VP}}$, $a_\mu^{\text{had,LO VP}}$ and $a_\tau^{\text{had,LO VP}}$, whereas the fifth and last columns list the contributions to $\Delta\alpha_{\text{had}}^{(5)}(M_Z^2)$ and $\Delta\nu_{\text{Mu}}^{\text{had,VP}}$, respectively. The last row describes the total contribution obtained from the sum of the individual final states, with the uncertainties added in quadrature.

Channel	$a_e^{\text{had,LO VP}} \times 10^{14}$	$a_\mu^{\text{had,LO VP}} \times 10^{10}$	$a_\tau^{\text{had,LO VP}} \times 10^{8}$	$\Delta\alpha_{\text{had}}^{(5)}(M_Z^2) \times 10^{4}$	$\Delta\nu_{\text{Mu}}^{\text{had,VP}}$ (Hz)
Chiral perturbation theory (ChPT) threshold contributions					
$\pi^0\gamma$	0.04 ± 0.00	0.12 ± 0.01	0.03 ± 0.00	0.00 ± 0.00	0.04 ± 0.00
$\pi^+\pi^-$	0.31 ± 0.01	0.87 ± 0.02	0.11 ± 0.00	0.01 ± 0.00	0.25 ± 0.01
$\pi^+\pi^-\pi^0$	0.00 ± 0.00	0.01 ± 0.00	0.00 ± 0.00	0.00 ± 0.00	0.00 ± 0.00
$\eta\gamma$	0.00 ± 0.00	0.00 ± 0.00	0.00 ± 0.00	0.00 ± 0.00	0.00 ± 0.00
Exclusive channels ($\sqrt{s} \leq 1.937$ GeV)					
$\pi^0\gamma$	1.19 ± 0.03	4.46 ± 0.10	1.75 ± 0.04	0.36 ± 0.01	1.45 ± 0.03
$\pi^+\pi^-$	138.59 ± 0.54	503.46 ± 1.91	172.84 ± 0.61	34.29 ± 0.12	159.64 ± 0.60
$\pi^+\pi^-\pi^0$	12.29 ± 0.25	46.73 ± 0.94	20.47 ± 0.39	4.69 ± 0.09	15.48 ± 0.31
$\pi^+\pi^-\pi^+\pi^-$	3.67 ± 0.05	14.87 ± 0.20	11.50 ± 0.16	4.02 ± 0.05	5.58 ± 0.08
$\pi^+\pi^-\pi^0\pi^0$	4.80 ± 0.19	19.39 ± 0.78	14.56 ± 0.58	5.00 ± 0.20	7.22 ± 0.29
$(2\pi^+2\pi^-\pi^0)_{\text{no }\eta\omega}$	0.24 ± 0.02	0.98 ± 0.09	0.84 ± 0.08	0.32 ± 0.03	0.38 ± 0.03
$(\pi^+\pi^-3\pi^0)_{\text{no }\eta}$	0.15 ± 0.03	0.62 ± 0.11	0.54 ± 0.10	0.21 ± 0.04	0.24 ± 0.04
$(3\pi^+3\pi^-)_{\text{no }\omega}$	0.06 ± 0.00	0.23 ± 0.01	0.21 ± 0.01	0.09 ± 0.01	0.09 ± 0.01
$(2\pi^+2\pi^-2\pi^0)_{\text{no }\eta}$	0.33 ± 0.04	1.35 ± 0.17	1.24 ± 0.15	0.51 ± 0.06	0.53 ± 0.07
$(\pi^+\pi^-4\pi^0)_{\text{no }\eta}$	0.05 ± 0.05	0.21 ± 0.21	0.19 ± 0.19	0.08 ± 0.08	0.08 ± 0.08
$(3\pi^+3\pi^-\pi^0)_{\text{no }\eta\omega}$	0.00 ± 0.00	0.00 ± 0.01	0.00 ± 0.00	0.00 ± 0.00	0.00 ± 0.00
K^+K^-	5.86 ± 0.06	23.03 ± 0.22	12.82 ± 0.12	3.37 ± 0.03	8.01 ± 0.08
$K_S^0K_L^0$	3.33 ± 0.05	13.04 ± 0.19	7.00 ± 0.10	1.77 ± 0.03	4.51 ± 0.07
$KK\pi$	0.66 ± 0.03	2.71 ± 0.12	2.33 ± 0.10	0.89 ± 0.04	1.05 ± 0.05
$KK2\pi$	0.47 ± 0.02	1.93 ± 0.08	1.80 ± 0.07	0.75 ± 0.03	0.76 ± 0.03
$KK3\pi$	0.01 ± 0.00	0.04 ± 0.02	0.04 ± 0.02	0.02 ± 0.01	0.02 ± 0.01
$\eta\gamma$	0.18 ± 0.01	0.70 ± 0.02	0.35 ± 0.01	0.09 ± 0.00	0.24 ± 0.01
$\eta\pi^+\pi^-$	0.33 ± 0.01	1.34 ± 0.05	1.10 ± 0.04	0.41 ± 0.02	0.51 ± 0.02
$(\eta\pi^+\pi^-\pi^0)_{\text{no }\omega}$	0.17 ± 0.02	0.71 ± 0.08	0.63 ± 0.07	0.25 ± 0.03	0.28 ± 0.03
$\eta2\pi^+2\pi^-$	0.02 ± 0.00	0.08 ± 0.01	0.07 ± 0.01	0.03 ± 0.00	0.03 ± 0.00
$\eta\pi^+\pi^-\pi^0\pi^0$	0.03 ± 0.00	0.12 ± 0.02	0.11 ± 0.02	0.05 ± 0.01	0.05 ± 0.01
$\eta\omega$	0.07 ± 0.01	0.30 ± 0.02	0.26 ± 0.02	0.10 ± 0.01	0.11 ± 0.01
$\omega(\to\pi^0\gamma)\pi^0$	0.22 ± 0.00	0.88 ± 0.02	0.61 ± 0.01	0.19 ± 0.00	0.32 ± 0.01
$\omega(\to\text{npp})2\pi$	0.03 ± 0.00	0.13 ± 0.01	0.12 ± 0.01	0.04 ± 0.00	0.05 ± 0.01
$\omega(\to\text{npp})3\pi$	0.04 ± 0.01	0.17 ± 0.03	0.15 ± 0.03	0.06 ± 0.01	0.07 ± 0.01
$\omega2\pi^+2\pi^-$	0.00 ± 0.00	0.01 ± 0.00	0.01 ± 0.00	0.00 ± 0.00	0.00 ± 0.00
$\eta\phi$	0.10 ± 0.00	0.41 ± 0.02	0.37 ± 0.02	0.15 ± 0.01	0.16 ± 0.01
$\omega\eta\pi^0$	0.06 ± 0.01	0.24 ± 0.05	0.23 ± 0.05	0.10 ± 0.02	0.10 ± 0.02
$\omega(\to\text{npp})KK$	0.00 ± 0.00	0.00 ± 0.00	0.00 ± 0.00	0.00 ± 0.00	0.00 ± 0.00
$\eta(\to\text{npp})KK_{\text{no }\phi\to KK}$	0.00 ± 0.00	0.01 ± 0.01	0.01 ± 0.01	0.01 ± 0.00	0.01 ± 0.01
$\phi \to$ unaccounted	0.01 ± 0.01	0.04 ± 0.04	0.02 ± 0.02	0.01 ± 0.01	0.01 ± 0.01
$p\bar{p}$	0.01 ± 0.00	0.03 ± 0.00	0.03 ± 0.00	0.01 ± 0.00	0.01 ± 0.00
$n\bar{n}$	0.01 ± 0.00	0.03 ± 0.01	0.03 ± 0.01	0.01 ± 0.00	0.01 ± 0.00
Other contributions ($\sqrt{s} > 1.937$ GeV)					
Inclusive channel	10.38 ± 0.16	43.55 ± 0.67	63.49 ± 0.91	82.78 ± 1.05	19.82 ± 0.30
J/ψ	1.49 ± 0.05	6.26 ± 0.19	8.91 ± 0.27	7.07 ± 0.22	2.81 ± 0.09
ψ'	0.37 ± 0.01	1.58 ± 0.04	2.50 ± 0.06	2.51 ± 0.06	0.74 ± 0.02
$\Upsilon(1S)$	0.01 ± 0.00	0.05 ± 0.00	0.12 ± 0.00	0.55 ± 0.02	0.03 ± 0.00
$\Upsilon(2S)$	0.00 ± 0.00	0.02 ± 0.00	0.05 ± 0.00	0.24 ± 0.01	0.01 ± 0.00
$\Upsilon(3S)$	0.00 ± 0.00	0.01 ± 0.00	0.03 ± 0.00	0.17 ± 0.01	0.01 ± 0.00
$\Upsilon(4S)$	0.00 ± 0.00	0.01 ± 0.00	0.02 ± 0.00	0.10 ± 0.01	0.00 ± 0.00
pQCD ($\sqrt{s} > 11.199$ GeV)	0.48 ± 0.00	2.07 ± 0.00	5.33 ± 0.00	124.79 ± 0.09	1.34 ± 0.00
Total ($<\infty$GeV)	186.08 ± 0.66	692.78 ± 2.42	332.81 ± 1.39	276.09 ± 1.12	232.04 ± 0.82

TABLE II. Summary of the contributions to $a_e^{\rm SM}$. The values of $a_e^{\rm QED}$ from $\alpha_{\rm Rb}$ (left) and $\alpha_{\rm Cs}$ (right) and their resulting values for $a_e^{\rm SM}$ and Δa_e are listed individually for comparison. All results are given as $a_e^{\rm SM} \times 10^{12}$.

SM contribution	$a_e(\alpha_{\rm Rb}) \times 10^{12}$		$a_e(\alpha_{\rm Cs}) \times 10^{12}$
QED	1159652180.309 ± 0.720 [11]		1159652179.887 ± 0.230 [14]
EW		0.031 ± 0.000 [11]	
had LO VP		1.861 ± 0.007 [12]	
had NLO VP		−0.223 ± 0.001 [12]	
had NNLO VP		0.028 ± 0.000 [11]	
had LbL		0.037 ± 0.005 [11]	
Theory total	1159652182.042 ± 0.720		1159652181.620 ± 0.230
Experiment		1159652180.730 ± 0.280 [10]	
Δa_e	−1.312 ± 0.773(1.7σ)		−0.890 ± 0.362(2.5σ)

been added linearly. Compared to $a_e^{\rm had}({\rm NT12}) = (167.8 \pm 1.4) \times 10^{-14}$ in Ref. [17], the mean value found in this work is outside the quoted error given in Ref. [17]. However, it should be noted that no determination of the NNLO hadronic VP contributions was available for Ref. [17], whereas in this work the addition of $a_e^{\rm had,NNLO\,VP} = (2.80 \pm 0.01) \times 10^{-14}$ constitutes, similar to the case of the muon, a significant additional correction.

The EW contributions, $a_e^{\rm EW} = (3.053 \pm 0.023) \times 10^{-14}$, are also taken from Ref. [47]. For the QED contributions, there are now two options depending on the choice for the value of α.[5] As described in Sec. I, the use of the measurement of α from Rb atomic interferometry [13] or Cs atomic interferometry [14] leads to an interesting comparison with $a_e^{\rm exp}$. For each case, the values of $a_e^{\rm QED}$ are

$$a_e^{\rm QED}(\alpha_{\rm Rb}) = (115965218030.9 \pm 72.0) \times 10^{-14} \, [11],$$
$$a_e^{\rm QED}(\alpha_{\rm Cs}) = (115965217988.7 \pm 23.0) \times 10^{-14} \, [14]. \quad (3.4)$$

Using these and the contributions from the EW and hadronic sectors, the SM predictions for a_e are found here to be

$$a_e^{\rm SM}(\alpha_{\rm Rb}) = (1159652182.042 \pm 0.72) \times 10^{-12},$$
$$a_e^{\rm SM}(\alpha_{\rm Cs}) = (1159652181.620 \pm 0.23) \times 10^{-12}. \quad (3.5)$$

The comparison of these results with the experimental measurement of a_e [10] is given in Table II and shown in Fig. 7. The values of the deviation between theory and experiment of $\Delta a_e(\alpha_{\rm Rb}) = (-1.31 \pm 0.77) \times 10^{-12}(1.7\sigma)$ and $\Delta a_e(\alpha_{\rm Cs}) = (-0.89 \pm 0.36) \times 10^{-12}(2.5\sigma)$ confirm the findings in Ref. [11] and Ref. [14], respectively.

B. The anomalous magnetic moment of the muon, a_μ

For the hadronic VP contribution to a_μ, at LO this analysis finds

---

[5]For the contributions from all the other sectors of the SM, the changes from the choice of α are negligible.

$$a_\mu^{\rm had,LO\,VP} = (692.78 \pm 1.21_{\rm stat} \pm 1.97_{\rm sys} \pm 0.21_{\rm vp}$$
$$\pm 0.70_{\rm fsr}) \times 10^{-10}$$
$$= (692.78 \pm 2.42_{\rm tot}) \times 10^{-10}, \quad (3.6)$$

and the NLO contributions are determined here to be

$$a_\mu^{\rm had,NLO\,VP} = (-9.83 \pm 0.01_{\rm stat} \pm 0.03_{\rm sys} \pm 0.01_{\rm vp}$$
$$\pm 0.02_{\rm fsr}) \times 10^{-10}$$
$$= (-9.83 \pm 0.04_{\rm tot}) \times 10^{-10}. \quad (3.7)$$

These results are consistent with the KNT18 analysis. At LO, the integral over the hadronic R-ratio determined in Ref. [1] resulted in $a_\mu^{\rm had,LOVP}({\rm KNT18}) = (693.26 \pm 2.46) \times 10^{-10}$. Comparing this with Eq. (3.6), the reduction in the mean value comes entirely from the updated treatment of the ω resonance in the $\pi^+\pi^-\pi^0$ channel described in Sec. II B. This change counteracts the small increase in the mean
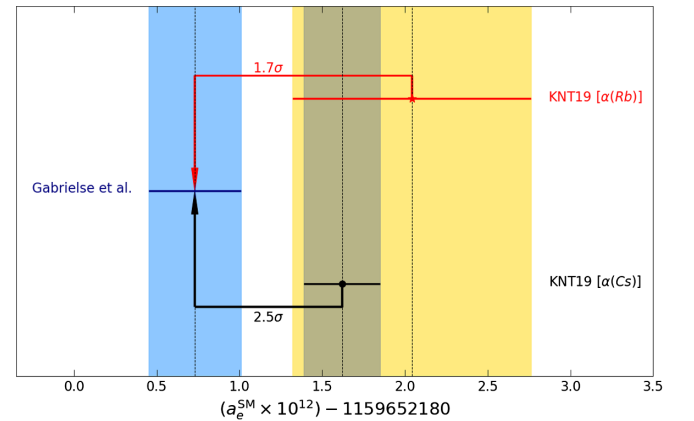

FIG. 7. A comparison of the evaluations of $a_e^{\rm SM}$ as determined in this work with the experimental measurement by Gabrielse et al. [10], the uncertainty of which is given by the light blue band. The red marker and yellow band denote the determination of $a_e^{\rm SM}$ using $\alpha_{\rm Rb}$, while the black marker and grey band denote the determination of $a_e^{\rm SM}$ using $\alpha_{\rm Cs}$ [for the values see Eq. (3.5) or Table II].
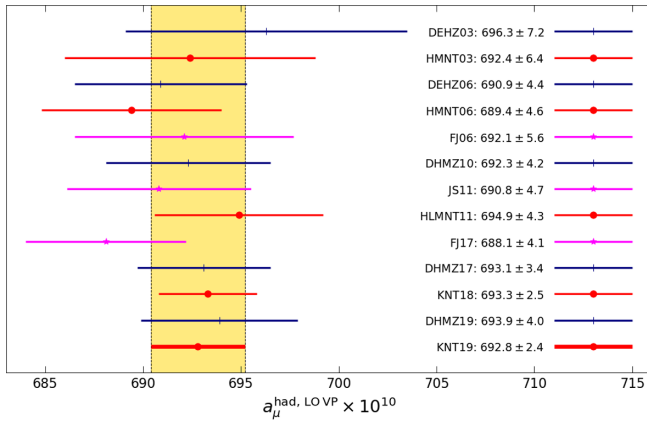
FIG. 8. Comparison of recent and previous evaluations of $a_\mu^{\text{had,LO VP}}$ determined from $e^+e^- \to$ hadrons cross section data. The analyses listed in chronological order are DEHZ03 [48], HMNT03 [22], DEHZ06 [49], HMNT06 [39], FJ06 [50], DHMZ10 [51], JS11 [52], HLMNT11 [40], FJ17 [53], DHMZ17 [54], KNT18 [1] and DHMZ19 [37]. The prediction from this work is listed as KNT19 and defines the (yellow) uncertainty band shown for the comparison with the other analyses.

value from the $\pi^+\pi^-$ channel due to the inclusion of the CLEO-c data [25] detailed in Sec. II A, as well as the very small increase due to the newly included channels reported in Sec. II C. The marginal decrease in the overall uncertainty is also due to the inclusion of the CLEO-c data [25], which as explained previously has caused a small decrease in the local χ^2 error inflation of the dominant two-pion contribution. A comparison of this result with similar evaluations of $a_\mu^{\text{had,LO VP}}$ determined from $e^+e^- \to$ hadrons cross section data is shown in Fig. 8. It is important to note that there is clear stability and overall agreement between the different analyses/groups over the consecutive years, despite the contrasting choices the different groups have made concerning how to treat the hadronic cross section data, where to use perturbative QCD (pQCD) instead of data and the application of other possible theoretical constraints.[6]

Combining the results (3.6) and (3.7) with the NNLO corrections, $a_\mu^{\text{had,NNLO VP}} = (1.24 \pm 0.01) \times 10^{-10}$ [24], the total hadronic VP contribution to a_μ is estimated to be

$$a_\mu^{\text{had,VP}} = (684.19 \pm 2.38_{\text{tot}}) \times 10^{-10}, \qquad (3.8)$$

---

[6]The most recent update from DHMZ19 has a larger uncertainty compared to that of DHMZ17, since DHMZ19 have included an additional error to account for the difference they obtained for $a_\mu^{\pi^+\pi^-}$ when discarding either the KLOE or the BABAR data. As the KNT $\pi^+\pi^-$ data combination benefits from stronger constraints imposed by the correlated uncertainties, the difference observed in $a_\mu^{\pi^+\pi^-}$ when discarding the data from either experiment is less severe. Therefore, and remembering also that data tensions are quantitatively accounted for in the resulting cross section by the local χ^2 error inflation, no additional uncertainty for a_μ is applied in this analysis.

where, as in the case of the electron, the errors have been added linearly due to the full correlation between the R-ratio input for the three contributions. When considering the SM prediction, in the case of the muon ($l = \mu$), the other contributions in Eq. (1.1) require reconsideration. In contrast to the case of the electron, the muon is, at the current level of accuracy, not sensitive to the choice of either $\alpha(\text{Rb})$ or $\alpha(\text{Cs})$, or the updated five-loop QED contributions from Ref. [11]. Hence the value of the QED contributions, to the accuracy needed and quoted here, is unchanged at $a_\mu^{\text{QED}} = (11658471.90 \pm 0.01) \times 10^{-10}$ [11,55]. For the EW contributions, the value chosen here is also the same as in Ref. [1]. However, it should be noted that an independent numerical evaluation of the two-loop EW contributions was recently performed [56], resulting in an estimate of the total EW contributions of $a_\mu^{\text{EW}} = (15.29 \pm 0.10) \times 10^{-10}$. This is consistent with the previously chosen value of $a_\mu^{\text{EW}} = (15.36 \pm 0.10) \times 10^{-10}$ [57] and therefore no adjustment is made for this analysis.

For the hadronic LbL sector, in Ref. [1] the commonly quoted "Glasgow consensus" estimate of $a_\mu^{\text{had,LbL}}(\text{"Glasgow consensus"}) = (10.5 \pm 2.6) \times 10^{-10}$ [58] was used, adjusted for a reevaluation of the contribution to $a_\mu^{\text{had,LbL}}$ due to axial exchanges [59–61]. This led to $a_\mu^{\text{had,LbL}} = (9.8 \pm 2.6) \times 10^{-10}$ [61] being adopted for the KNT18 analysis. Since that time, the progress in determining $a_\mu^{\text{had,LbL}}$ using dispersive approaches (where dispersion relations are formulated that allow for the determination of the hadronic LbL contributions from experimental data) has been significant.[7] These determinations are of particular interest for this analysis, as the fundamental approach to this work (and the works preceding it [1,22,39,40]) is that any estimates given should be as model independent and/or as data driven as possible. With the contributions to the "Glasgow consensus" estimate having been solely determined through model-dependent approaches, moving towards data-based evaluations of the hadronic LbL contributions is consistent with the general methodology of this undertaking.

Those hadronic LbL contributions that have been determined by dispersive techniques are the pseudoscalar poles (π^0, η, η') [62–64], the pion/kaon-box contributions [9,65] and the S-wave $\pi\pi$ rescattering contributions [65,66]. In addition, a new analysis of (longitudinal) short-distance constraints has very recently become available [67,68], complementing the dispersive determination of the pseudoscalar contributions. The values for these contributions and their counterparts from the "Glasgow consensus" estimate are shown in Table III, where the estimate of

---

[7]This advancement has been largely influenced by the efforts of the Muon $g - 2$ Theory Initiative [9] and the commendable work and successes of the groups within it, which have formed the basis for the following choices for $a_\mu^{\text{had,LbL}}$ made in this work.

TABLE III. Comparison of the contributions to $a_\mu^{\mathrm{had,LbL}}$ from the "Glasgow consensus" estimate and from recent evaluations mainly based on dispersive approaches. The single column results from the scalars, tensors and axial-vectors originate from the "Glasgow consensus" estimate. The total uncertainty for the value including the dispersive evaluations is determined via the conservative linear sum of the errors of the individual contributions. All results are given as $a_\mu^{\mathrm{had,LbL}} \times 10^{11}$.

Contribution	'Glasgow consensus' [58]		Dispersive evaluations
π^0, η, η' poles	114 ± 13		93.8 ± 4.0 [62–64]
π/K box	-19 ± 19		-16.4 ± 0.2 [9,65]
S-wave $\pi\pi$ rescattering	$\cdots$		-8 ± 1 [65,66]
Short-distance contributions	[Part of π^0, η, η' poles]		13 ± 6 [67,68]
Charm contributions	2.3		3 ± 1 [67,68]
Scalars and tensors		-7 ± 7	
Axial-vectors		15 ± 10	
Total	105 ± 26		93.4 ± 29.2

TABLE IV. Summary of the contributions to a_μ^{SM}.

SM contribution	$a_\mu \times 10^{10}$
QED	11658471.90 ± 0.01 [11]
EW	15.36 ± 0.10 [57]
had LO VP	692.78 ± 2.42
had NLO VP	-9.83 ± 0.04
had NNLO VP	1.24 ± 0.01 [24]
had LO LbL	9.34 ± 2.92
had NLO LbL	0.30 ± 0.20 [70]
Theory total	11659181.08 ± 3.78
Experiment	11659209.10 ± 6.33 [5]
Δa_μ	$28.02 \pm 7.37 (3.80\sigma)$

the pseudoscalar contributions of the "Glasgow consensus" already contains short-distance contributions. With the aim to strive for a more model-independent approach, the value for $a_\mu^{\mathrm{had,LbL}}$ in this work is taken as the sum of the contributions determined via dispersive approaches, the new estimates of short-distance and charm quark corrections, plus the sum of the contributions from scalars, tensors and axial-vectors remaining from the original "Glasgow consensus" estimate.[8] This results in a value for the total hadronic LbL contribution of $a_\mu^{\mathrm{had,LbL}} = (9.34 \pm 2.92) \times 10^{-10}$, where the errors from the individual contributions have been summed linearly. This provides a conservative estimate of the overall uncertainty and also accounts for currently unavailable transverse short-distance constraints, which are estimated to be subleading.

The values for the contributions from all the individual sectors of the SM chosen in this analysis are summarized in Table IV. Summing these contributions together results in

an updated SM prediction of the anomalous magnetic moment of the muon of

$$a_\mu^{\mathrm{SM}} = (11\,659\,181.08 \pm 3.78) \times 10^{-10}, \quad (3.9)$$

where the uncertainty is determined from the uncertainties of the individual SM contributions added in quadrature. This value deviates from the current experimental measurement [5] by

$$\Delta a_\mu = (28.02 \pm 7.37) \times 10^{-10}, \quad (3.10)$$

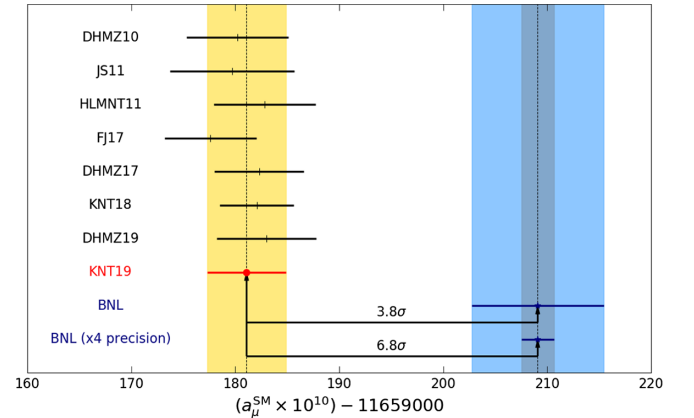corresponding to a muon $g-2$ discrepancy of 3.8σ. This result is compared with other determinations of a_μ^{SM} in

FIG. 9. A comparison of recent and previous evaluations of a_μ^{SM}. The analyses listed in chronological order are DHMZ10 [51], JS11 [52], HLMNT11 [40], FJ17 [53] and DHMZ17 [54], KNT18 [1] and DHMZ19 [37]. The prediction from this work is listed as KNT19, which defines the uncertainty band that other analyses are compared to. The current uncertainty on the experimental measurement [2–5] is given by the light blue band. The light grey band represents the hypothetical situation of the new experimental measurement at Fermilab yielding the same mean value for a_μ^{exp} as the BNL measurement, but achieving the projected fourfold improvement in its uncertainty [6].

---

[8]Note that the adjustments of the axial contributions mentioned above and adopted in Ref. [1], have recently been found to be not justified (see Ref. [69]), and hence the estimate for the axial contributions from the original "Glasgow consensus" is used here.

TABLE V. Summary of the contributions to a_τ^{SM}.

SM contribution	a_τ
QED	$(117324.0 \pm 2.0) \times 10^{-8}$ [19]
EW	$(47.4 \pm 0.5) \times 10^{-8}$ [19]
had LO VP	$(332.8 \pm 1.4) \times 10^{-8}$
had NLO VP	$(7.9 \pm 0.0) \times 10^{-8}$
had LbL	$(5.0 \pm 3.0) \times 10^{-8}$ [19]
Theory total	$(117717.1 \pm 3.9) \times 10^{-8}$
Experiment	-0.018 ± 0.017 [18]
Δa_τ	$-0.019 \pm 0.017 \ (-1.1\sigma)$

Fig. 9. The value for a_μ^{SM} in Eq. (3.9) has decreased by 0.96×10^{-10} compared to the KNT18 analysis [1]. This change comes, in nearly equal parts, from the reduction in the mean value of $a_\mu^{\mathrm{had,LO\,VP}}$ and the new estimate of $a_\mu^{\mathrm{had,LbL}}$ in this work. The increase in the uncertainty with respect to Ref. [1] comes from the increase in the error of $a_\mu^{\mathrm{had,LbL}}$ owing to the changes in the estimate of this contribution discussed previously. Together, these have resulted in the increased discrepancy from 3.7σ in the KNT18 analysis to 3.8σ in this work.

C. The anomalous magnetic moment of the tau lepton, a_τ

In the case of the τ, the determination of the LO hadronic VP contributions yields

$$
\begin{aligned}
a_\tau^{\mathrm{had,LO\,VP}} &= (332.81 \pm 0.47_{\mathrm{stat}} \pm 1.09_{\mathrm{sys}} \pm 0.17_{\mathrm{vp}} \\
&\quad \pm 0.69_{\mathrm{fsr}}) \times 10^{-8} \\
&= (332.81 \pm 1.39_{\mathrm{tot}}) \times 10^{-8},
\end{aligned} \tag{3.11}
$$

while at NLO they are found to be

$$
\begin{aligned}
a_\tau^{\mathrm{had,NLO\,VP}} &= (7.85 \pm 0.01_{\mathrm{stat}} \pm 0.03_{\mathrm{sys}} \pm 0.01_{\mathrm{vp}} \\
&\quad \pm 0.02_{\mathrm{fsr}}) \times 10^{-8} \\
&= (7.85 \pm 0.04_{\mathrm{tot}}) \times 10^{-8}.
\end{aligned} \tag{3.12}
$$

Note that in the case of the τ, the total NLO contributions are positive, while they are negative for the electron and muon, and any estimate based on a naive mass scaling of the result for the muon would fail completely. The results for $a_\tau^{\mathrm{had,LO\,VP}}$ from the individual hadronic channels are given in Table I. Comparing with the evaluation in Ref. [19], which resulted in $a_\tau^{\mathrm{had,LO\,VP}} = (337.5 \pm 3.7) \times 10^{-8}$, and $a_\tau^{\mathrm{had,NLO\,VP}} = (7.6 \pm 0.2) \times 10^{-8}$ obtained already in Ref. [23], there is consistency between the mean values found in the different analyses. However, there is a large reduction in the error in this work which is mainly due to the abundance of precise new data since [19]. Utilizing the values from Ref. [19] for the QED, EW and hadronic LbL contributions

(listed in Table V), the updates to the hadronic VP contributions result in a SM prediction for the anomalous magnetic moment of the tau lepton of

$$
a_\tau^{\mathrm{SM}} = (117717.1 \pm 3.9) \times 10^{-8}. \tag{3.13}
$$

With the uncertainties of the hadronic VP contributions significantly improved, the uncertainty of a_τ^{SM} is now dominated by the hadronic LbL contributions, which account for $\sim 60\%$ of the total error. However, it should be noted that the QED contributions, at $\sim 26\%$ of the total error, are now less precise than the hadronic VP contributions. As explained in Ref. [19], the entire error $\delta a_\tau^{\mathrm{QED}} \sim 2 \times 10^{-8}$ is assigned as the uncertainty due to the missing contributions at four-loop order (and beyond), and are crudely estimated from logarithmically enhanced terms expected at the four-loop level. This indicates that a calculation of a_τ^{QED} at four loops would significantly improve the determination of a_τ^{SM}.

Although, as stated in Sec. I, the precision of the current experimental measurement of $a_\tau^{\mathrm{exp}} = -0.018(17)$ [18] makes a meaningful comparison between theory and experiment futile, this analysis confirms a difference $\Delta a_\tau = a_\tau^{\mathrm{exp}} - a_\tau^{\mathrm{SM}}$ at the level of 1σ as found in Ref. [18]. While at present there seems little prospect for an experiment dedicated to measuring a_τ, it is not impossible to imagine that this might become feasible in the future. Indeed, the additional potential for new physics discoveries due to the higher mass scale of the τ compared to the electron or the muon make this an interesting consideration.

D. Determination of $\alpha(M_Z^2)$

The running (scale-dependent) QED coupling, $\alpha(q^2)$, is determined via $\alpha(q^2) = \alpha/(1 - \Delta\alpha_{\mathrm{had}}(q^2) - \Delta\alpha_{\mathrm{lep}}(q^2))$, where the contributions to the running are separated into hadronic (had) and leptonic (lep) components. Of the three fundamental EW parameters of the SM [the Fermi constant G_F, M_Z and $\alpha(M_Z^2)$], the effective QED coupling at the Z boson mass, $\alpha(M_Z^2)$, is the least precisely known, where the uncertainties from the nonperturbative, hadronic contributions limit the accuracy of EW precision fits. The five-flavor (all quark flavors except the top quark which can be treated perturbatively) contributions to $\alpha(M_Z^2)$ are determined from the dispersion relation

$$
\Delta\alpha_{\mathrm{had}}^{(5)}(M_Z^2) = -\frac{\alpha M_Z^2}{3\pi} \mathrm{P} \int_{s_{th}}^{\infty} \mathrm{d}s \, \frac{R(s)}{s(s - M_Z^2)}, \tag{3.14}
$$

where P indicates the principal value of the integral. Using the updated compilation for $R(s)$ from this work, and perturbative QCD for energies $\sqrt{s} > 11.199$ GeV (above the thresholds for all five quark flavors), this data-driven evaluation gives the result

TABLE VI. Comparison of recent and previous evaluations of $\Delta\alpha_{\mathrm{had}}^{(5)}(M_Z^2)$ determined from $e^+e^- \to$ hadrons cross section data and the corresponding results for $\alpha^{-1}(M_Z^2)$.

Analysis	$\Delta\alpha_{\mathrm{had}}^{(5)}(M_Z^2) \times 10^4$	$\alpha^{-1}(M_Z^2)$
DHMZ10 [51]	275.59 ± 1.04	128.952 ± 0.014
HLMNT11 [40]	276.26 ± 1.38	128.944 ± 0.019
FJ17 [47]	277.38 ± 1.19	128.919 ± 0.022
DHMZ17 [54]	276.00 ± 0.94	128.947 ± 0.012
KNT18	276.11 ± 1.11	128.946 ± 0.015
DHMZ19 [37]	276.10 ± 1.00	128.946 ± 0.013
KNT19 [This work]	276.09 ± 1.12	128.946 ± 0.015

$$\Delta\alpha_{\mathrm{had}}^{(5)}(M_Z^2) = (276.09 \pm 0.26_{\mathrm{stat}} \pm 0.68_{\mathrm{sys}} \pm 0.14_{\mathrm{vp}}$$
$$\pm\, 0.83_{\mathrm{fsr}}) \times 10^{-4}$$
$$= (276.09 \pm 1.12_{\mathrm{tot}}) \times 10^{-4}. \qquad (3.15)$$

From this, the total value of the QED coupling at the Z boson mass is

$$\alpha^{-1}(M_Z^2) = (1 - \Delta\alpha_{\mathrm{lep}}(M_Z^2) - \Delta\alpha_{\mathrm{had}}^{(5)}(M_Z^2) - \Delta\alpha_{\mathrm{top}}(M_Z^2))\alpha^{-1}$$
$$= 128.946 \pm 0.015, \qquad (3.16)$$

updating the result from Ref. [1]. As in Ref. [1], the leptonic contribution is $\Delta\alpha_{\mathrm{lep}}(M_Z^2) = (314.979 \pm 0.002) \times 10^{-4}$ [71,72]. The contribution from the top quark is updated from Refs. [73,74] by using $m_t = 172.9(0.4)$ GeV, $\alpha_s(M_Z) = 0.1181(11)$ [2] and by including the contributions from $\mathcal{O}(\alpha_s^0 m_Z^6/m_t^6)$ and $\mathcal{O}(\alpha_s^1 m_Z^6/m_t^6)$ terms which were neglected in Ref. [74]. This results in $\Delta\alpha_{\mathrm{top}}(M_Z^2) = (-0.7201 \pm 0.0037) \times 10^{-4}$. A comparison with previous, largely data-driven determinations of $\Delta\alpha_{\mathrm{had}}^{(5)}(M_Z^2)$ and $\alpha^{-1}(M_Z^2)$ is given in Table VI.

E. The hyperfine splitting of muonium, $\Delta\nu_{\mathrm{Mu}}^{\mathbf{had,VP}}$

For many years, precision measurements of the ground-state HFS of muonium $\Delta\nu_{\mathrm{Mu}}$ served as a rigorous test of QED. Today, it still provides the best approach for determining the value of the electron-to-muon mass ratio and, therefore, the muon mass. Like the lepton $g-2$, $\Delta\nu_{\mathrm{Mu}}$ is sensitive to quantum effects, and thus any differences in the comparison of experimental and theoretical determinations could be an indication of new physics. The current most precise experimental measurements of $\Delta\nu_{\mathrm{Mu}}$ [75,76] result in

$$\Delta\nu_{\mathrm{Mu}}^{\mathrm{exp}} = (4463302776 \pm 51)\ \mathrm{Hz}. \qquad (3.17)$$

With the most recent of these measurements having been performed more than 20 years ago, the MuSEUM experiment at J-PARC is currently in the process of measuring the HFS of muonium (and the electron-to-muon mass ratio)

with an aim to reduce the uncertainty in Eq. (3.17) by an order of magnitude [77].

The theoretical prediction, $\Delta\nu_{\mathrm{Mu}}^{\mathrm{SM}}$, as given by CODATA 2014 [78],[9] is

$$\Delta\nu_{\mathrm{Mu}}^{\mathrm{SM}}(\mathrm{CODATA}) = (4463302868 \pm 271)\ \mathrm{Hz}. \qquad (3.18)$$

Although the HFS of muonium is mainly QED dominated, it receives higher-order contributions from the EW and hadronic sectors. In the case of the hadronic contributions, the hadronic LO VP contributions are dominant, while the hadronic LbL contributions are negligible compared to the current level of precision [$\Delta\nu_{\mathrm{Mu}}^{\mathrm{had,LbL}} \simeq 0.0065(10)$ Hz [78,80]]. The CODATA determination given in Eq. (3.18) currently utilizes the value for the hadronic LO VP contributions that was determined in the NT12 analysis preceding this work [17], which found

$$\Delta\nu_{\mathrm{Mu}}^{\mathrm{had,VP}}(\mathrm{NT12}) = (232.68 \pm 1.44)\ \mathrm{Hz}. \qquad (3.19)$$

These contributions can be determined via the dispersion integral

$$\Delta\nu_{\mathrm{Mu}}^{\mathrm{had,VP}} = \frac{1}{2\pi^3}\frac{m_e}{m_\mu}\nu_F \int_{m_{\pi^0}^2}^{\infty} ds\, K_{\mathrm{Mu}}(s)\sigma_{\mathrm{had},\gamma}^0(s). \qquad (3.20)$$

Here, ν_F denotes the so-called Fermi energy,

$$\nu_F = \frac{16}{3}R_\infty\alpha^2\frac{m_e}{m_\mu}\left[1 + \frac{m_e}{m_\mu}\right]^{-3}, \qquad (3.21)$$

where R_∞ is the Rydberg constant. The kernel function $K_{\mathrm{Mu}}(s)$ was described in detail in Ref. [17].

Now utilizing the compilation of the hadronic cross section determined in this work (see Sec. II), the updated value for the hadronic VP contributions to the ground-state HFS of muonium is found to be

$$\Delta\nu_{\mathrm{Mu}}^{\mathrm{had,VP}} = (232.04 \pm 0.38_{\mathrm{stat}} \pm 0.66_{\mathrm{sys}}$$
$$\pm\, 0.08_{\mathrm{vp}} \pm 0.27_{\mathrm{fsr}})\ \mathrm{Hz}$$
$$= (232.04 \pm 0.82_{\mathrm{tot}})\ \mathrm{Hz}. \qquad (3.22)$$

Here, a noticeable mean value reduction and an uncertainty reduction of $\sim 43\%$ compared to Eq. (3.19) are observed, which is in accordance with the same trends seen in the development of the corresponding determinations of a_μ over the same period. Adjusting the theoretical prediction in Eq. (3.18) for this value results in

---

[9]Note that in Ref. [79] it was claimed that the uncertainty in Eq. (3.18) is underestimated by a factor of $\sim 1/2$ due to the implicit assumption that there is no new physics beyond the SM in relations used by the CODATA estimate. The theoretical (th) prediction in Ref. [79] reads $\Delta\nu_{\mathrm{Mu}}^{\mathrm{th}} = (4463302872 \pm 515)$ Hz.

$$\Delta\nu_{\mathrm{Mu}}^{\mathrm{SM}} = (4463302867 \pm 271)\ \mathrm{Hz}, \qquad (3.23)$$

which, despite the noticeable changes in $\Delta\nu_{\mathrm{Mu}}^{\mathrm{had,VP}}$ between this work and the previous analysis, highlights the minimal impact of the hadronic contributions to this observable compared to the dominant QED contributions.

IV. CONCLUSIONS AND FUTURE PROSPECTS

This analysis, KNT19, has presented updated evaluations of the hadronic vacuum polarization contributions to the anomalous magnetic moments of the electron ($a_e^{\mathrm{had,VP}}$), muon ($a_\mu^{\mathrm{had,VP}}$) and tau lepton ($a_\tau^{\mathrm{had,VP}}$), to the ground-state hyperfine splitting of muonium ($\Delta\nu_{\mathrm{Mu}}^{\mathrm{had,VP}}$), and has also updated the value of the hadronic contributions to the running of the QED coupling at the scale of the mass of the Z boson [$\Delta\alpha_{\mathrm{had}}(M_Z^2)$]. These quantities are calculated using the hadronic R-ratio, obtained from a compilation of all available $e^+e^- \rightarrow$ hadrons cross section data. In this work, the data compilation has been updated from the determination in Ref. [1], accounting for new measurements. In the dominant $\pi^+\pi^-$ channel, the inclusion of the CLEO-c data [25] has increased the mean value slightly and marginally improved the uncertainty of $a_\mu^{\pi^+\pi^-}$. In the $\pi^+\pi^-\pi^0$ channel, adjustments have been made to the treatment of the narrow ω resonance, which is now integrated over using a quintic polynomial interpolation in order to avoid an overestimation of the cross section from a linear interpolation that was recently noted in Ref. [38]. This has reduced the mean value of $a_\mu^{\pi^+\pi^-\pi^0}$ by $\sim 1 \times 10^{-10}$ and, in turn, contributed to a significant reduction of the mean value of a_μ^{SM} in this work, although it is important to note that all estimates from this analysis are consistent with those given in Ref. [1]. In addition, other new measurements have been included which have removed the need to rely on isospin relations to estimate cross sections in three subleading channels, where in each case the new data agree well with the predictions of the KNT18 analysis.

The resulting hadronic R-ratio has been used as input into dispersion relations to determine $a_l^{\mathrm{had,VP}}$ ($l = e, \mu, \tau$) at LO and NLO, $\Delta\alpha_{\mathrm{had}}(M_Z^2)$ and $\Delta\nu_{\mathrm{Mu}}^{\mathrm{had,VP}}$. This work has found $\Delta\alpha_{\mathrm{had}}^{(5)}(M_Z^2) = (276.09 \pm 1.12_{\mathrm{tot}}) \times 10^{-4}$ which has yielded a value for the QED coupling at the Z boson mass of $\alpha^{-1}(M_Z^2) = 128.946 \pm 0.015$, which is consistent with Ref. [1]. For the hadronic VP contributions to the ground-state hyperfine splitting of muonium, the new data compilation gives $\Delta\nu_{\mathrm{Mu}}^{\mathrm{had,VP}} = (232.04 \pm 0.82_{\mathrm{tot}})$ Hz, which is consistent with the previous determination of this quantity in Ref. [17], but constitutes a significant uncertainty reduction of $\sim 43\%$. A similar error reduction has been observed in the determination of the anomalous magnetic moment of the electron compared to Ref. [17], with this analysis finding $a_e^{\mathrm{had,LOVP}} = (186.08 \pm 0.66_{\mathrm{tot}}) \times 10^{-14}$. This, coupled with new estimates for the NLO contributions,

TABLE VII. Comparison of the contributions to $a_l^{\mathrm{had,LO\,VP}}$ and a_l^{SM} as determined in this work. All results are presented in units of $a_l \times 10^7$ in order to compare the relevant magnitudes and precision of the various contributions. In this instance, the value of a_e^{SM} corresponds to a_e^{QED} determined using α_{Rb}.

Lepton flavor, l	$a_l^{\mathrm{had,LO\,VP}} \times 10^7$	$a_l^{\mathrm{SM}} \times 10^7$
e	0.00001861(7)	11596.52182042(720)
μ	0.69278(242)	11659.18108(378)
τ	33.281(139)	11771.71(39)

translates to differences between experiment and theory of $\Delta a_e(\alpha_{\mathrm{Rb}}) = (-1.312 \pm 0.773) \times 10^{-12}$ (1.7σ) and $\Delta a_e(\alpha_{\mathrm{Cs}}) = (-0.890 \pm 0.362) \times 10^{-12}$ (2.5σ), depending on whether the QED contributions are determined using α measured via Rb or Cs atomic interferometry. For the muon $g-2$, the new KNT19 analysis gives $a_\mu^{\mathrm{had,LO\,VP}} = (692.78 \pm 2.42_{\mathrm{tot}}) \times 10^{-10}$ and $a_\mu^{\mathrm{had,NLO\,VP}} = (-9.83 \pm 0.04_{\mathrm{tot}}) \times 10^{-10}$. New choices in this work for the hadronic LbL contributions based on recent results from dispersive approaches (which have already significantly consolidated the "Glasgow consensus"), coupled with the contributions from the other sectors of the SM, have resulted in a new estimate for the Standard Model prediction of $a_\mu^{\mathrm{SM}} = (11659181.08 \pm 3.78) \times 10^{-10}$, which deviates from the current experimental measurement by 3.8σ. In the case of the τ, the value at LO is $a_\tau^{\mathrm{had,LO\,VP}} = (332.81 \pm 1.39_{\mathrm{tot}}) \times 10^{-8}$, consistent with the value found in Ref. [19], but with an uncertainty that is smaller by $\sim 62\%$. Unfortunately, the current experimental bounds of the measured value of a_τ are not stringent enough to draw any strong conclusions from the comparison between experiment and theory.

It is interesting to compare the values and uncertainties of $a_l^{\mathrm{had,LO\,VP}}$ and a_l^{SM} of the different leptons, which are shown in Table VII. Here, especially in the case of the hadronic contributions, the difference in the resulting magnitudes of these values due to lepton mass-scaling arguments is evident. Indeed, in the most extreme example, the value of $a_l^{\mathrm{had,LO\,VP}}$ is $\mathcal{O}(10^6)$ times larger for the τ than for the electron. For a_l^{SM}, the most striking difference is in the level of the precision between the different leptons. The electron, being less sensitive to hadronic effects than the muon or the τ, is by far the most precise. However, the larger uncertainty of a_τ^{SM} compared to a_μ^{SM} is not solely due to hadronic contributions (where, for the muon, the hadronic LbL estimates are more accurate than for the τ). Instead, as noted in Sec. III C, the uncertainty assigned due to the missing four-loop contributions is a main cause of this disparity and could be improved through the calculation of a_τ^{QED} at four-loop order.

With the tantalizing prospect of new experimental measurements of a_μ from Fermilab in the near future,

and later from J-PARC, the predictions of $a_\mu^{\mathrm{had,VP}}$ and a_μ^{SM} have been reexamined in detail and found to be robust. The opportunity to further improve the hadronic VP contributions estimated by dispersive approaches (as in this analysis) largely rests on new hadronic cross section measurements. For the $\pi^+\pi^-$ channel, new measurements currently under analysis from the CMD-3, SND and *BABAR* experiments are eagerly awaited. Although these measurements are important in terms of improving the overall precision of $a_\mu^{\mathrm{had,VP}}$, it is hoped that they will help to resolve the lingering deviation between the KLOE [28–31] and *BABAR* [32] measurements, which drive the data tensions in $a_\mu^{\pi^+\pi^-}$. In addition, expected data for the $\pi^+\pi^-\pi^0$, $\pi^+\pi^-\pi^0\pi^0$ and the inclusive channels, will be very beneficial. In preparation for the new experimental measurements of a_μ, the efforts of the Muon $g-2$ Theory Initiative [9] (and the groups within it) have already led to impressive achievements with regards to advancing the determinations of the hadronic VP and hadronic LbL contributions. Of great interest are the results from lattice QCD, which already provide first-principles cross checks of the now very precise data-driven estimates for the hadronic contributions to a_μ^{SM}. These are expected to become competitive with the current determinations within the next few years. Given the continued advancements in the theoretical predictions of a_μ, coupled with the substantial progress of the experimental community, the study of the muon anomalous magnetic moment has never been better placed to

severely constrain many scenarios for new physics beyond the SM, or, should the muon $g-2$ discrepancy become fully established, to claim a discovery of new physics.

[1] A. Keshavarzi, D. Nomura, and T. Teubner, Phys. Rev. D **97**, 114025 (2018).

[2] M. Tanabashi *et al.* (Particle Data Group), Phys. Rev. D **98**, 030001 (2018) and 2019 update.

[3] G. W. Bennett *et al.* (Muon g-2 Collaboration), Phys. Rev. Lett. **89**, 101804 (2002); **89**, 129903(E) (2002).

[4] G. W. Bennett *et al.* (Muon g-2 Collaboration), Phys. Rev. Lett. **92**, 161802 (2004).

[5] G. W. Bennett *et al.* (Muon g-2 Collaboration), Phys. Rev. D **73**, 072003 (2006).

[6] J. Grange *et al.* (Muon g-2 Collaboration), arXiv:1501.06858.

[7] A. Keshavarzi (Muon g-2 Collaboration), EPJ Web Conf. **212**, 05003 (2019).

[8] M. Abe *et al.*, Prog. Theor. Exp. Phys. **2019**, 053C02 (2019).

[9] The Muon $g-2$ Theory Initiative, https://indico.fnal.gov/event/13795/, https://indico.him.uni-mainz.de/event/11/, http://www.int.washington.edu/PROGRAMS/19-74W/.

[10] D. Hanneke, S. Fogwell, and G. Gabrielse, Phys. Rev. Lett. **100**, 120801 (2008).

[11] T. Aoyama, T. Kinoshita, and M. Nio, Phys. Rev. D **97**, 036001 (2018).

[12] T. Aoyama, M. Hayakawa, T. Kinoshita, and M. Nio, Phys. Rev. Lett. **109**, 111807 (2012).

[13] R. Bouchendira, P. Clade, S. Guellati-Khelifa, F. Nez, and F. Biraben, Phys. Rev. Lett. **106**, 080801 (2011).

[14] R. H. Parker, C. Yu, W. Zhong, B. Estey, and H. Müller, Science **360**, 191 (2018).

[15] S. Volkov, Phys. Rev. D **100**, 096004 (2019).

[16] A. Crivellin, M. Hoferichter, and P. Schmidt-Wellenburg, Phys. Rev. D **98**, 113002 (2018).

[17] D. Nomura and T. Teubner, Nucl. Phys. **B867**, 236 (2013).

[18] J. Abdallah *et al.* (DELPHI Collaboration), Eur. Phys. J. C **35**, 159 (2004).

[19] S. Eidelman and M. Passera, Mod. Phys. Lett. A **22**, 159 (2007).

[20] S. J. Brodsky and E. de Rafael, Phys. Rev. **168**, 1620 (1968).

[21] B. E. Lautrup and E. de Rafael, Phys. Rev. **174**, 1835 (1968).

[22] K. Hagiwara, A. D. Martin, D. Nomura, and T. Teubner, Phys. Rev. D **69**, 093003 (2004).

[23] B. Krause, Phys. Lett. B **390**, 392 (1997).

[24] A. Kurz, T. Liu, P. Marquard, and M. Steinhauser, Phys. Lett. B **734**, 144 (2014).

[25] T. Xiao, S. Dobbs, A. Tomaradze, K. K. Seth, and G. Bonvicini, Phys. Rev. D **97,** 032012 (2018).
[26] F. Jegerlehner, https://www-com.physik.hu-berlin.de/~fjeger/alphaQEDn.uu (2003).
[27] A. Keshavarzi, D. Nomura, and T. Teubner (to be published).
[28] F. Ambrosino et al. (KLOE Collaboration), Phys. Lett. B **670,** 285 (2009).
[29] F. Ambrosino et al. (KLOE Collaboration), Phys. Lett. B **700,** 102 (2011).
[30] D. Babusci et al. (KLOE Collaboration), Phys. Lett. B **720,** 336 (2013).
[31] A. Anastasi et al. (KLOE-2 Collaboration), J. High Energy Phys. 03 (2018) 173.
[32] B. Aubert et al. (BABAR Collaboration), Phys. Rev. Lett. **103,** 231801 (2009).
[33] G. Colangelo, M. Hoferichter, and P. Stoffer, J. High Energy Phys. 02 (2019) 006.
[34] B. Ananthanarayan, I. Caprini, and D. Das, Phys. Rev. D **98,** 114015 (2018).
[35] B. Ananthanarayan, I. Caprini, D. Das, and I. Sentitemsu Imsong, Phys. Rev. D **89,** 036007 (2014).
[36] B. Ananthanarayan, I. Caprini, D. Das, and I. Sentitemsu Imsong, Phys. Rev. D **93,** 116007 (2016).
[37] M. Davier, A. Hoecker, B. Malaescu, and Z. Zhang, arXiv:1908.00921.
[38] M. Hoferichter, B. L. Hoid, and B. Kubis, J. High Energy Phys. 08 (2019) 137.
[39] K. Hagiwara, A. D. Martin, D. Nomura, and T. Teubner, Phys. Lett. B **649,** 173 (2007).
[40] K. Hagiwara, R. Liao, A. D. Martin, D. Nomura, and T. Teubner, J. Phys. G **38,** 085003 (2011).
[41] M. N. Achasov et al., Phys. Rev. D **98,** 112001 (2018).
[42] J. P. Lees et al. (BABAR Collaboration), Phys. Rev. D **98,** 112015 (2018).
[43] S. S. Gribanov et al., arXiv:1907.08002.
[44] M. N. Achasov et al., Phys. Rev. D **99,** 112004 (2019).
[45] V. L. Ivanov et al., Phys. Lett. B **798,** 134946 (2019).
[46] R. R. Akhmetshin et al. (CMD-3 Collaboration), Phys. Lett. B **792,** 419 (2019).
[47] F. Jegerlehner, EPJ Web Conf. **218,** 01003 (2019).
[48] M. Davier, S. Eidelman, A. Höcker, and Z. Zhang, Eur. Phys. J. C **31,** 503 (2003).
[49] M. Davier, Nucl. Phys. B, Proc. Suppl. **169,** 288 (2007).
[50] F. Jegerlehner, Nucl. Phys. B, Proc. Suppl. **162,** 22 (2006).
[51] M. Davier, A. Hoecker, B. Malaescu, and Z. Zhang, Eur. Phys. J. C **71,** 1515 (2011); **72,** 1874(E) (2012).
[52] F. Jegerlehner and R. Szafron, Eur. Phys. J. C **71,** 1632 (2011).
[53] F. Jegerlehner, EPJ Web Conf. **166,** 00022 (2018).
[54] M. Davier, A. Hoecker, B. Malaescu, and Z. Zhang, Eur. Phys. J. C **77,** 827 (2017).
[55] T. Aoyama, M. Hayakawa, T. Kinoshita, and M. Nio, Phys. Rev. Lett. **109,** 111808 (2012).
[56] T. Ishikawa, N. Nakazawa, and Y. Yasui, Phys. Rev. D **99,** 073004 (2019).
[57] C. Gnendiger, D. Stöckinger, and H. Stöckinger-Kim, Phys. Rev. D **88,** 053005 (2013).
[58] J. Prades, E. de Rafael, and A. Vainshtein, Adv. Ser. Dir. High Energy Phys. **20,** 303 (2009).
[59] F. Jegerlehner, EPJ Web Conf. **118,** 01016 (2016).
[60] V. Pauk and M. Vanderhaeghen, Eur. Phys. J. C **74,** 3008 (2014).
[61] A. Nyffeler, Phys. Rev. D **94,** 053006 (2016).
[62] M. Hoferichter, B. L. Hoid, B. Kubis, S. Leupold, and S. P. Schneider, Phys. Rev. Lett. **121,** 112002 (2018).
[63] P. Masjuan and P. Sanchez-Puertas, Phys. Rev. D **95,** 054026 (2017).
[64] M. Hoferichter, B. L. Hoid, B. Kubis, S. Leupold, and S. P. Schneider, J. High Energy Phys. 10 (2018) 141.
[65] G. Colangelo, M. Hoferichter, M. Procura, and P. Stoffer, J. High Energy Phys. 04 (**2017**) 161.
[66] G. Colangelo, M. Hoferichter, M. Procura, and P. Stoffer, Phys. Rev. Lett. **118,** 232001 (2017).
[67] G. Colangelo, F. Hagelstein, M. Hoferichter, L. Laub, and P. Stoffer, arXiv:1910.13432.
[68] G. Colangelo, F. Hagelstein, M. Hoferichter, L. Laub, and P. Stoffer, arXiv:1910.11881.
[69] M. Hoferichter at the INT Workshop INT-19-74W, University of Washington, WA (US), https://indico.fnal.gov/event/21626/session/9/contribution/49/material/slides/0.pdf.
[70] G. Colangelo, M. Hoferichter, A. Nyffeler, M. Passera, and P. Stoffer, Phys. Lett. B **735,** 90 (2014).
[71] M. Steinhauser, Phys. Lett. B **429,** 158 (1998).
[72] C. Sturm, Nucl. Phys. **B874,** 698 (2013).
[73] K. G. Chetyrkin, J. H. Kühn, and M. Steinhauser, Phys. Lett. B **371,** 93 (1996); Nucl. Phys. **B482,** 213 (1996); **505,** 40 (1997).
[74] J. H. Kühn and M. Steinhauser, Phys. Lett. B **437,** 425 (1998).
[75] F. G. Mariam et al., Phys. Rev. Lett. **49,** 993 (1982).
[76] W. Liu et al., Phys. Rev. Lett. **82,** 711 (1999).
[77] P. Strasser et al., Hyperfine Interact. **237,** 124 (2016).
[78] P. J. Mohr, D. B. Newell, and B. N. Taylor, Rev. Mod. Phys. **88,** 035009 (2016).
[79] M. I. Eides, Phys. Lett. B **795,** 113 (2019).
[80] S. G. Karshenboim, V. A. Shelyuto, and A. I. Vainshtein, Phys. Rev. D **78,** 065036 (2008).